

# An Algorithm to Produce Temporally and Spatially Continuous MODIS-LAI Time Series

Feng Gao, *Member, IEEE*, Jeffrey T. Morisette, Robert E. Wolfe, Greg Ederer, Jeff Pedelty, Edward Masuoka, Ranga Myneni, Bin Tan, and Joanne Nightingale

**Abstract**—Ecological and climate models require high-quality consistent biophysical parameters as inputs and validation sources. NASA’s Moderate Resolution Imaging Spectroradiometer (MODIS) biophysical products provide such data and have been used to improve our understanding of climate and ecosystem changes. However, the MODIS time series contains occasional lower quality data, gaps from persistent clouds, cloud contamination, and other gaps. Many modeling efforts, such as those used in the North American Carbon Program, that use MODIS data as inputs require gap-free data. This letter presents the algorithm used within the MODIS production facility to produce temporally smoothed and spatially continuous biophysical data for such modeling applications. We demonstrate the algorithm with an example from the MODIS-leaf-area-index (LAI) product. Results show that the smoothed LAI agrees with high-quality MODIS LAI very well. Higher  $R$ -squares and better linear relationships have been observed when high-quality retrieval in each individual tile reaches 40% or more. These smoothed products show similar data quality to MODIS high-quality data and, therefore, can be substituted for low-quality retrievals or data gaps.

**Index Terms**—Biophysical parameters, gap filling, Moderate Resolution Imaging Spectroradiometer (MODIS) land products, remote sensing, time-series data analysis.

## I. INTRODUCTION

THE MODERATE Resolution Imaging Spectroradiometer (MODIS) is a key instrument aboard NASA’s Terra and Aqua satellites. Terra MODIS and Aqua MODIS image the entire Earth’s surface every one to two days and provide vital information for global-change research. MODIS land products, such as leaf area index (LAI) and fraction of photosynthetically active radiation, are critical inputs to parameterize or validate climate and ecosystem process models [1].

The MODIS-LAI product has been validated with independent field measurements [2] but, generally, under clear-sky conditions (see the MODIS-land-validation Web site <http://landval.gsfc.nasa.gov>).

Manuscript received April 27, 2007; revised August 16, 2007. This work was supported by the National Aeronautics and Space Administration (NASA) Advancing Collaborative Connections for Earth–Sun System Science (ACCESS) under NASA Task 05-ACCESS/05-44.

F. Gao is with Earth Resources Technology, Inc., Annapolis Junction, MD 20701 USA, with the Beijing Normal University, Beijing 100875, China, and also with the Terrestrial Information Systems Branch, NASA Goddard Space Flight Center, Greenbelt, MD 20771 USA (e-mail: fgao@ltpmail.gsfc.nasa.gov).

J. T. Morisette, R. E. Wolfe, J. Pedelty, E. Masuoka, B. Tan, and J. Nightingale are with the Terrestrial Information Systems Branch, NASA Goddard Space Flight Center, Greenbelt, MD 20771 USA.

G. Ederer is with the Science Applications International Corporation (SAIC), Seabrook, MD 20706 USA, and also with the Terrestrial Information Systems Branch, NASA Goddard Space Flight Center, Greenbelt, MD 20771 USA.

R. Myneni is with the Department of Geography, Boston University, Boston, MA 02215 USA.

Digital Object Identifier 10.1109/LGRS.2007.907971

However, cloud contamination, persistent clouds, and other suboptimal atmospheric or illumination conditions can reduce data quality and cause missing data in MODIS multiday land products. Although the MODIS-LAI product will produce results even under cloudy or suboptimal condition, care is taken to use the MODIS quality-assessment (QA) data layers to flag these values as lower or poor quality [1]. However, this is not acceptable for those ecosystem or climate models requiring realistic, high-quality, temporally, and spatially continuous measurements, such as the models being used in the North American Carbon Program (NACP).

This letter describes a procedure for producing temporally smoothed and spatially complete MODIS data sets. The procedure contains two algorithm stages, one for smoothing and one for gap filling, which attempt to maximize the use of high-quality data to replace missing or poor-quality observations. The algorithm uses an augmented version of the TIMESAT software [3], [4] for interpolation.

We start by describing the algorithm and then by presenting the results for the MODIS-LAI product, followed by the summary conclusions and a brief discussion of future plans.

## II. ALGORITHM DEVELOPMENT

The TIMESAT program was developed by Jonsson and Eklundh [3], [4] for analyzing time-series satellite-sensor data. This program provides the following three different smoothing functions to fit the time-series data: asymmetric Gaussian (AG); double logistic (DL); and adaptive Savitzky–Golay (SG) filtering. The adaptive SG-filtering approach uses local polynomial functions in fitting. It can capture subtle and rapid changes in the time series but is also sensitive to noise. Both AG and DL approaches use semilocal methods. They are less sensitive to the noise and can give a better description on the beginnings and endings of the seasons [4]. TIMESAT has been used successfully to analyze the vegetation index (VI) from time-series Advanced Very High Resolution Radiometer (AVHRR) data [4]. Zhang *et al.* [5] developed a fitting approach independently using a similar DL function and applied it to the MODIS time-series data successfully. Beck *et al.* [6] examined both the DL- and AG-function approaches and found that the use of either a DL function or an AG function is appropriate for describing vegetation dynamics at high latitudes. They also found that the DL functions describe the normalized difference vegetation index (NDVI) data better than both the Fourier series and the AG functions, as quantified by the root-mean-square errors [6]. We tested both the AG and DL approaches in the TIMESAT program and found that they produced similar results, with the exception that the AG approach is less sensitive to the

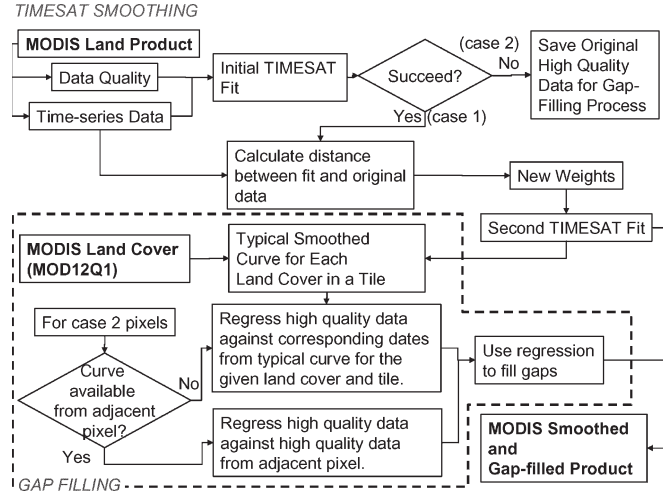


Fig. 1. Flow diagram of the TIMESAT temporal-fitting and gap-filling (dashed box) procedure.

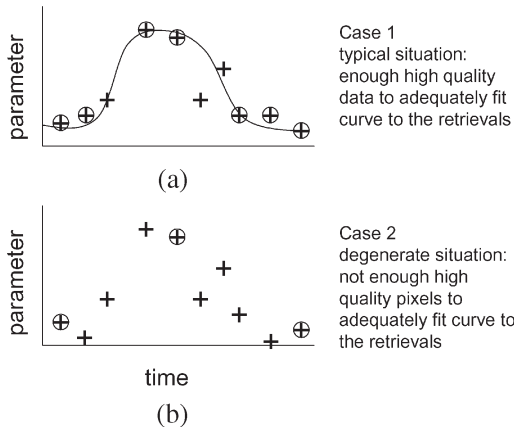


Fig. 2. Examples of the original time-series (crosses) and high-quality values (circled crosses) and the temporal-curve fitting (line).

incomplete time-series data with many data gaps in our experiments. We used the AG approach in this letter.

The flow diagram for the augmented TIMESAT procedure is given in Fig. 1. We start with a given continuous MODIS land-product time series and its associated QA-information time series. TIMESAT provides a weighting mechanism such that some values in the time series can be more influential than others. The initial work with the TIMESAT calculated the weights for AVHRR-NDVI values by considering cloud screening [4] using the thresholds of the AVHRR reflectance and thermal channels [7]. For our algorithm, the initial weights are based entirely on the MODIS QA layers associated with a given MODIS product. We assign high weights for higher quality retrievals and low weights for lower quality retrievals.

After the initial fit from TIMESAT, the algorithm takes one of the two branches based on the quality of the fit (represented by the “Succeed?” diamond in Fig. 1). The majority of the pixels follow the first branch [Fig. 2(a)] where there are enough high-quality observations to allow TIMESAT to fit a curve to the time series. The second branch is followed if there are too many gaps or low-quality data [Fig. 2(b)]. In this case, TIMESAT fails to fit a curve to the time series; therefore, we apply a gap-filling strategy. A successful run of TIMESAT

requires that there is no missing time period longer than 0.2 years and that there are less than 25% missing values over the entire time series (three years).

*Case 1—Successful TIMESAT Fit:* After applying the TIMESAT fitting with the initial weights, we adjust the weights based on the fitted results from the first iteration for a second pass through the TIMESAT fitting. The revised data weights for the second run through the TIMESAT are based on the scaled difference between the original data and the fitted value. Specifically, the new weights are

$$w' = w \left[ 1 / \left( 1 + \frac{|dy|}{S\sigma} \right) \right],$$

if  $dy \leq 0$  (MODIS value is below TIMESAT curve) (1)

$$w' = w \left( 1 + \frac{|dy|}{S\sigma} \right),$$

if  $dy > 0$  (MODIS value is above TIMESAT curve) (2)

where  $dy$  is the difference between the original MODIS value and the TIMESAT-fitted values,  $\sigma$  is the standard deviation of  $\{dy_i\}$  (standard deviation of residuals from the first fitting, where  $i$  represents all high-quality data), and  $S$  is a constant parameter for the weight adjustment.

This process is similar to the upper envelope weighting scheme in the TIMESAT software [3], which forces the curve to fit upper values more closely. The upper envelope option has been tested for VI and is very effective because high parameter values normally represent clear-sky conditions or better viewing or illumination geometry [3]. Similar to VI, higher LAI values normally represent retrievals under clear-sky conditions since cloud contamination tends to reduce reflectance in near-infrared band and to increase in red band and thus leads to lower LAI retrievals. Because cloud contamination tends to reduce the value of vegetation-related parameters, the weight is decreased if a TIMESAT-fitted value is larger than the retrieved parameter and vice versa. This enables the TIMESAT fit to more closely follow the upper envelope of the retrieved parameter values. Note that only the weights for the MODIS high-quality data are adjusted in our processing. The weights for the low-quality data remain the same. We did not use the existing upper envelope option in the TIMESAT software since we need a better control on the initial weights passed from the MODIS data-quality flags.

*Case 2—TIMESAT Failure to Fit and Gap-Filling Algorithm:* The TIMESAT program can only produce fitted values if there are enough high-quality data in the time series. No result will be produced if there are too many missing values because the fitting function becomes unreliable if it is forced to do so. In addition, some fits may be unrealistic (e.g., out of the data range) due to noise or limitations of the fitting function. In these cases, instead of trying to fit a curve to the smaller number of high-quality data points, we use a separate gap-filling process.

Our gap-filling algorithm is represented within the dashed line in Fig. 1. The algorithm uses two major steps. First, it searches an appropriate seasonal-variation curve for the gap. Second, it adjusts the seasonal-variation curve to the sparsely available high-quality observations of the gap.

For the first step, we developed two strategies for establishing an appropriate seasonal-variation curve. In the first strategy,

the algorithm searches for the pixels with the same land-cover type (from MOD12Q) within a small window around the pixel. Within these nearby pixels, the algorithm checks if there are any “case 1,” the successful TIMESAT temporal curves. If more than one “case 1” pixel is found, we choose the one with the highest quality from all candidates. We start with a small search window ( $11 \times 11$  MODIS 1-km pixels). If such a pixel is not available either due to too many gaps or to no matching land-cover type, the program automatically increases the search-window size. We set the number of pixels on the next new search to be equal to the number of pixels on the previous test. If a seasonal-variation curve cannot be located within the defined maximum search distance ( $120 \times 120$  MODIS 1-km pixels or about  $1^\circ$ ), then the second strategy is used for this pixel. In the second strategy, the algorithm averages all high-quality seasonal-variation curves for each land-cover type within a tile and builds a tile-level seasonal-variation pattern for each land-cover type. The tile-level seasonal variation of the same land-cover type is then used for this pixel. This process ensures that an appropriate TIMESAT seasonal curve can always be located, whether it is from a nearby pixel or from the tile-level seasonal curve. We refer to this chosen seasonal curve as the “ancillary seasonal curve.”

Once the ancillary seasonal curve  $f_n(t, c)$  is found, a regression transform function  $r(x)$  is computed such that the temporal-variation curve of the gap pixel can be computed using  $r(f_n(t, c))$ . The parameters of this transform function are determined strictly by the high-quality data pairs between the case-2 pixel with gaps and the ancillary seasonal curves using least square approach with cost function

$$M_g(t_i, c) = r(f_n(t_i, c)) + \varepsilon \quad (3)$$

where subscript  $n$  represents the neighbor pixel, subscript  $g$  represents the current gap pixel,  $t_i$  represents the  $i$ th production date,  $c$  represents the land-cover type,  $\varepsilon$  is the error between the gap and curve values,  $M_g(t_i, c)$  represents all the available high-quality MODIS data of the gap pixel, and  $f_n(t_i, c)$  is the TIMESAT seasonal-variation curve from the neighbor pixel (strategy 1) or tile-level average (strategy 2). We use the second-order polynomial function for the computation, i.e.,  $r(x) = ax^2 + bx + c$ . The seasonal-variation curve  $f_g(t, c)$  of the gap pixel is computed using

$$f_g(t, c) = r(f_n(t, c)). \quad (4)$$

The algorithm allows flexibility in the time window used to compute the transfer function. In the extreme, the function can be fit with all the high-quality data pairs from the entire time series being considered. Alternatively, the algorithm can use a local window of high-quality data pairs within a subset period, centered on the date of the gap being filled. There is a tradeoff between having enough observations to fit the transfer function versus a small enough window to capture interannual data variations. In this letter, we used a one-year period as the local moving time window in a way that a gap pixel at each production date is computed from the two half-year periods before and after.

### III. INITIAL RESULTS

The algorithm is now discussed with an example using collection 4 (C4) MODIS-eight-day-LAI products from 2001 to 2005 as inputs to produce smoothed and gap-filled MODIS-LAI data for North America from 2001 to 2005. The final output includes three LAI layers and three QA layers. The three LAI layers include the original MODIS LAI, the smoothed and gap-filled LAI, and the composed LAI. The composed LAI uses high-quality LAI from the original MODIS product but replaces low-quality retrievals with smoothed and gap-filled LAI. Each layer has a corresponding QA layer.

The approach that we discussed previously is applicable to most tiles in North America. However, some high-latitude tiles need special attention because of too many missing values caused by extreme solar geometries during winter. For these tiles, we use the minimum snow-free LAI from all production periods to replace the missing or snow-covered values with initial weights the same as low-quality retrievals (0.25). Issues with snow cover warrant similar considerations for other applications or MODIS products.

Each LAI value is first weighted according to the quality flags embedded in the MODIS product. A summary of quality analysis and validation activities of the collection 3 (C3) MODIS-LAI product by Yang *et al.* [8] indicates an overestimation of LAI for all six biomes by about 12% (RMSE = 0.66). MODIS LAI retrieved from the radiative-transfer model (main algorithm) with the best quality can reach an accuracy of 0.3 LAI for cropland [8], [9] and 0.5 LAI for needleleaf forest [8], [10]. This overestimation of LAI has been addressed in C4 and was further refined in collection 5 (C5) processing [11], [12]. Generally, the quality-control flags embedded in the MODIS-LAI product reflect the retrieval quality reasonably well.

For MODIS-eight-day-LAI product (MOD15A2), the initial weights are assigned as follows.

- 1)  $w = 1.0$  for LAI retrievals from the radiative-transfer model (high quality) or for LAI retrieval that reaches saturation.
- 2)  $w = 0.25$  for retrievals from an empirical model.
- 3)  $w = 0.0$  for all invalid and fill values.

Saturated LAI values are assigned high weights since those values are normally retrieved under clear-sky condition and reach the limits of optical remote sensing. They represent high-quality values in our current approach.

Recall that, in our second iteration with the TIMESAT, only weights for high-quality data are adjusted in our processing. Weights for low-quality data remain the same. We use  $S = 2.0$  as our weighting-adjustment constant value. This means that, for the weights listed here, according to (1), there should be at least six standard-deviation differences between the original and the fitted values for a high-quality LAI retrieval ( $w = 1.0$ ) reduced to the same weight as a low-quality retrieval ( $w = 0.25$ ). We constrain the adjusted weight in the range of 0.25–4.0, which ensures that the MODIS high-quality retrievals still get higher weights than the low-quality retrievals even if they are below the TIMESAT curve from the first iteration.

Fig. 3 shows an example of the fittings from the DL-function and SG-filtering approaches and the two iterations of fitting LAI time-series data using the AG functions. We used all the available LAI data from 2001 to 2005. This site ( $86.7102^\circ$  W,

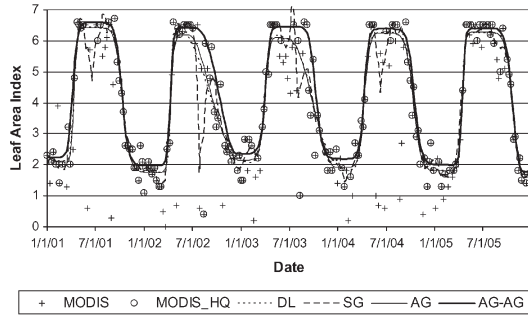


Fig. 3. Example of fitting MODIS-LAI data (crosses) with TIMESAT DL function (short-dashed line), SG filtering (long-dashed line), and AG function based on the following two different weighting schemes: the first time-fitting attempt (AG) based on LAI quality flags only (thin solid line) and the two-iteration approach (AG-AG) with a revised weighting scheme (thick solid line). The two-iteration approach shows a better fitting result to high LAI values, as well as high-quality data. High-quality retrievals (main algorithm) are highlighted in circles.

35.1625° N) shows a very good seasonal cycle of a typical deciduous broadleaf forest. In the figure, the short-dashed line and the long-dashed line represent results from the DL-function and SG-filtering approaches, respectively. The SG-filtering approach is sensitive to the noisy data in the summer season. The thin solid line represents the results from the first TIMESAT AG fit using weights based on the LAI quality flags. In this iteration, the high LAI values are underestimated even though the total fitting error is minimized particularly in the summer of 2002 and 2003 (same for the DL approach). The weights on the high-quality data are then adjusted based on the difference between the first fit and the original values. After the second iteration (AG-AG) using the revised weights, the fit results (thick solid line) capture high LAI values better. It also shows a more consistent five-year seasonal variation. The weights of the noisy data in the summer of 2002 and 2003 have been reduced and bring the fitted curve closer to the upper values.

As discussed in the MODIS-LAI-validation references [8]–[13], it is preferred that MODIS-LAI validation be performed at the patch scale. The same land-cover type within a patch size shows similar patterns of seasonal variation. Therefore, as discussed in Section II, it is reasonable to use the seasonal-variation pattern from a neighboring pixel with same MODIS biome type as an *a priori* information for a case-2 gap pixel. With this extra *a priori* information available, we scale the seasonal-variation curve to match the sparsely available high-quality LAI values. Moody *et al.* [14] used a similar approach to fill MODIS-albedo missing values from historical high-quality albedo data and temporal curves from neighbor pixels and produced a value-added MODIS-albedo data set successfully.

Fig. 4 shows a particularly challenging time series that was well characterized by our algorithm. The seasonal curve (solid line) is from a case-2 pixel (88.8395° W, 46.1125° N) fit using the seasonal-variation curve of a neighbor pixel with the same land-cover type (deciduous broadleaf forest, short-dashed line) and selected high-quality MODIS-LAI data (solid circles). In this example, our gap-filling approach captured the seasonal trend and fit to both high-quality (circled crosses) and low-quality (crosses only) MODIS retrievals well even though we only selected five high-quality data in the test.

Since MODIS high-quality LAI retrievals have been assessed and validated (as validated stage 1) via field measurements,

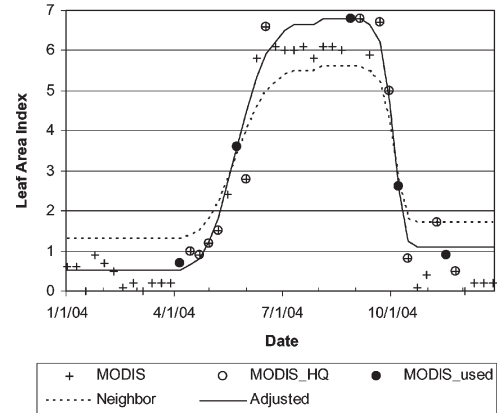


Fig. 4. Seasonal-variation curve from local adjustment gap-filling algorithm (solid line) captures seasonal trends from selected high-quality MODIS-LAI data (in solid circles) and seasonal-variation curve from a neighbor pixel with same land-cover type (deciduous broadleaf forest, short-dashed line).

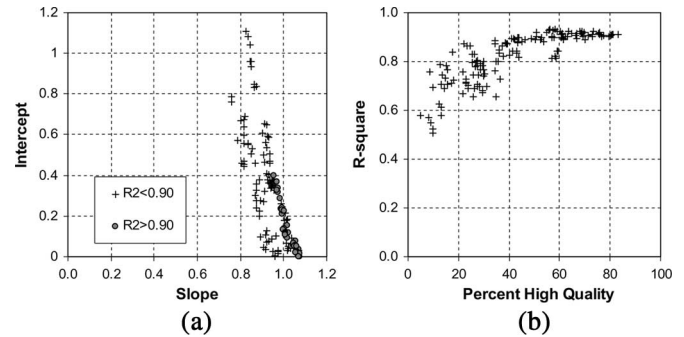


Fig. 5. Linear relationships of high-quality MODIS retrievals and smoothed LAI show a good agreement in the scatter plots (a) of slope and intercept and (b) of  $R^2$  and percentage high quality. Each point in the figure is computed based on one tile from one-year data. Note that the intercept is in LAI units.

we can validate the smoothed LAI data indirectly by comparing smoothed LAI to the high-quality MODIS-LAI product. Fig. 5(a) shows the scatter plot of the intercepts and slopes of the smoothed LAI and the MODIS high-quality LAI based on each tile. In the figure, each point represents the result of a tile from the high-quality MODIS retrievals and the smoothed LAI based on one year of LAI data. The point (intercept = 0, slope = 1.0) means a perfect match. This figure shows, generally, a good agreement between the MODIS high-quality LAI data and the smoothed LAI data, particularly for those tiles with higher  $R^2$  ( $> 0.9$ , filled circles in figure). The  $R^2$  plot based on the percentage of high-quality retrievals [Fig. 5(b)] reveals that a better agreement can be achieved if a high percentage of high-quality retrievals is available. The  $R$ -squares are all above 0.8 and reach as high as 0.9 when high-quality retrievals are 40% or more temporally and spatially within a tile in the fitting and gap-filling production period. There are about 50% tiles in the North America, which have 40% or more high-quality measurement.

Fig. 6(a) shows a scatter plot of the smoothed LAI versus all the high-quality MODIS LAI for North America tiles from the beginning of the four seasons (eight-day production periods starting from January 1, 2004, April 6, 2004, July 11, 2004, and October 15, 2004). The smoothed LAI has a very high correlation with the high-quality MODIS-LAI data with  $R^2 = 0.826$ , and the points fall close to the 1-to-1 line (slope = 0.998, intercept =  $-0.206$ ). We also did a cross comparison by taking

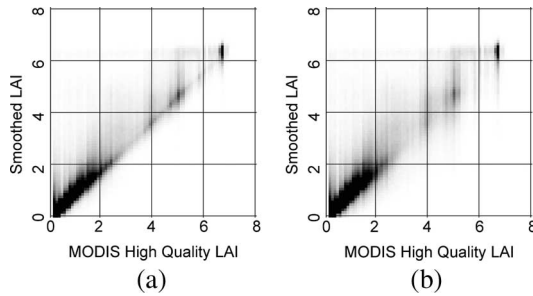


Fig. 6. Good agreement can be seen from the scatter plots of (a) all MODIS high-quality LAI and the smoothed LAI ( $y = 0.998x + 0.206$ ,  $R^2 = 0.826$ ) and (b) excluded MODIS high-quality LAI and the smoothed LAI ( $y = 0.966x + 0.230$ ,  $R^2 = 0.787$ ) based on North America tiles on January 1, 2004, April 6, 2004, July 11, 2004, and October 15, 2004.

out 10% of the MODIS high-quality values randomly from TIMESAT processing and then by comparing the smoothed results to the excluded high-quality data. Fig. 6(b) shows a scatter plot of the smoothed LAI versus the excluded high-quality data from the different seasons. The smoothed LAI shows slightly reduced but still a very high correlation with these excluded high-quality data (slope = 0.966, intercept = 0.230,  $R^2 = 0.787$ ). Since high-quality MODIS-LAI data in C4 have been validated and show good agreement with field measurements, Figs. 5 and 6 show that, in most cases, the smoothed and gap-filled LAIs have an accuracy similar to the original high-quality retrievals from the radiative-transfer approach. This also means that it is reasonable for the smoothed LAI to be substituted for low-quality retrievals or data gaps.

#### IV. CONCLUSION AND DISCUSSION

MODIS land products provide high-quality-data sources for climate, weather forecast, and ecological models. However, these products need to be further processed to remove data gaps and low-quality data caused by cloud contamination or algorithm limitations before they can be used in models directly. To archive this goal for the NACP, we developed an algorithm using the TIMESAT software to smooth and to gap-fill MODIS-LAI time-series data. For our example, comparisons between the MODIS high-quality LAI data and the smooth LAI data agree very well with an overall  $R^2 = 0.921$  for North America. The agreement of individual tiles (regions) depends on the number of high-quality retrievals within that tile. High  $R$ -squares and better linear relationships are observed when high-quality retrievals reach 40% or more. As the smoothed LAI product shows similar data quality to the MODIS high-quality LAI, it is therefore reasonable to substitute low-quality retrievals or gaps in the original MODIS data with the smoothed product.

Although the smoothed LAI product has a good agreement with MODIS high-quality data, they may not, however, agree with ground measurements particularly when there were large gaps in the time series during critical plant-growing stages (such as the short-peak summertime at high-latitude areas). Our current smoothing algorithm cannot capture seasonal variations if the MODIS data lack enough information. A future possible remedy would be to introduce historical data into the smoothing algorithm based on the assumption that temporal curves are similar year to year.

Results demonstrated in this letter are based on the MODIS C4 processing. As MODIS C5 products become available,

we will reprocess our products using the C5 data. Since our algorithm places an emphasis on MODIS high-quality data, improvements in C5 products should improve our smoothed products as well. Preliminary C5 processing for LAI indicates that there will be more high-quality retrievals even at higher latitudes. This is encouraging, given the results in Fig. 6, as more high-quality retrievals imply that our smoothed values are closer to a one-to-one agreement with the high-quality data.

In this letter, we successfully demonstrated temporal fitting and gap filling based on three- and five-year MODIS-LAI data over North America. In future production, we will use a three-year moving-window approach to produce a smoothed product for each of the middle years. We will continue our tests by including different ecosystem regions such as tropical and high-latitude regions for global applications and expand the application of the algorithm to other continuous MODIS land products.

#### ACKNOWLEDGMENT

The authors would like to thank Dr. N. Shabanov and the investigators from the NACP for the many discussions.

#### REFERENCES

- [1] R. B. Myneni, S. Hoffman, Y. Knyazikhin *et al.*, "Global products of vegetation leaf area and fraction absorbed PAR from year one of MODIS data," *Remote Sens. Environ.*, vol. 83, no. 1/2, pp. 214–231, Nov. 2002.
- [2] J. T. Morisette, J. L. Privette *et al.*, "A framework for the validation of MODIS land products," *Remote Sens. Environ.*, vol. 83, no. 1/2, pp. 77–96, Nov. 2002.
- [3] P. Jonsson and L. Eklundh, "TIMESAT—A program for analyzing time-series of satellite sensor data," *Comput. Geosci.*, vol. 30, no. 8, pp. 833–845, Oct. 2004.
- [4] P. Jonsson and L. Eklundh, "Seasonality extraction by function fitting to time-series of satellite sensor data," *IEEE Trans. Geosci. Remote Sens.*, vol. 40, no. 8, pp. 1824–1832, Aug. 2002.
- [5] X. Zhang, M. A. Friedl, C. B. Schaaf *et al.*, "Monitoring vegetation phenology using MODIS," *Remote Sens. Environ.*, vol. 84, no. 3, pp. 833–845.
- [6] P. S. A. Beck, C. Atzberger, K. A. Høgda *et al.*, "Improved monitoring of vegetation dynamics at very high latitudes: A new method using MODIS NDVI," *Remote Sens. Environ.*, vol. 100, no. 3, pp. 321–334, Feb. 2006.
- [7] L. L. Stowe, E. P. McClain, R. Carey *et al.*, "Global distribution of cloud cover derived from NOAA/AVHRR operational satellite data," *Adv. Space Res.*, vol. 11, no. 3, pp. 51–54, 1991.
- [8] W. Yang, B. Tan, D. Huang *et al.*, "MODIS leaf area index products: From validation to algorithm improvement," *IEEE Trans. Geosci. Remote Sens.*, vol. 44, no. 7, pp. 1885–1898, Jul. 2006.
- [9] B. Tan, J. Hu, P. Zhang *et al.*, "Validation of Moderate Resolution Imaging Spectroradiometer leaf area index product in croplands of Alpillies, France," *J. Geophys. Res.*, vol. 110, no. D1, pp. D01107.1–D01107.15, 2005. DOI:10.1029/2004JD004860.
- [10] Y. Wang, C. E. Woodcock, W. Buermann *et al.*, "Evaluation of the MODIS LAI algorithm at a coniferous forest site in Finland," *Remote Sens. Environ.*, vol. 91, no. 1, pp. 114–127, May 2004.
- [11] W. Yang, N. V. Shabanov, D. Huang *et al.*, "Analysis of leaf area index products from combination of MODIS Terra and Aqua data," *Remote Sens. Environ.*, vol. 104, no. 3, pp. 297–312, Oct. 2006.
- [12] N. V. Shabanov, D. Huang, W. Yang *et al.*, "Analysis and optimization of the MODIS leaf area index algorithm retrievals over broadleaf forests," *IEEE Trans. Geosci. Remote Sens.*, vol. 43, no. 8, pp. 1855–1865, Aug. 2005.
- [13] W. Yang, D. Huang, B. Tan *et al.*, "Analysis of leaf area index and fraction of PAR absorbed by vegetation products from the Terra MODIS sensor: 2000–2005," *IEEE Trans. Geosci. Remote Sens.*, vol. 44, no. 7, pp. 1829–1842, Jul. 2006.
- [14] E. G. Moody, M. D. King, S. P. Platnick *et al.*, "Spatially complete global spectral surface albedos: Value-added datasets derived from Terra MODIS land products," *IEEE Trans. Geosci. Remote Sens.*, vol. 43, no. 1, pp. 144–158, Jan. 2005.